

ASSESSMENT OF COMPUTATIONAL ISSUES  
ASSOCIATED WITH ANALYSIS OF HIGH-LIFT SYSTEMS

522-02

160482

N93-27449

R. Balasubramanian<sup>+</sup>  
Spectrex Inc., Gloucester, Virginia

and

Kenneth M. Jones<sup>++</sup> and Edgar G. Waggoner<sup>+++</sup>  
NASA Langley Research Center

Abstract

Thin-layer Navier-Stokes calculations for wing-fuselage configurations from subsonic to hypersonic flow regimes are now possible. However, efficient, accurate solutions for using these codes for two- and three dimensional high-lift systems have yet to be realized. A brief overview of salient experimental and computational research is presented. An assessment of the state-of-the-art relative to high-lift system analysis and identification of issues related to grid generation and flow physics which are crucial for computational success in this area are also provided. Research in support of the high-lift elements of NASA's High Speed Research and Advanced Subsonic Transport Programs which addresses some of the computational issues is presented. Finally, fruitful areas of concentrated research are identified to accelerate overall progress for high lift system analysis and design.

I. Introduction

An area of special interest to aerospace designers is high-lift systems. Future transport aircraft will have multiple requirements playing important roles in their design. These requirements include improved energy efficiency, reduced noise, and lower maintenance costs. Improved high-lift concepts for subsonic transports may result in designs which have increased section thicknesses, larger aspect ratios, lower sweeps, optimized multi-component designs, highly integrated propulsion systems, and integrated pneumatic concepts such as circulation control. Conversely, transports designed for supersonic cruise typically have geometric characteristics (highly swept, slender wings) which do not lend themselves to efficient aerodynamics at low subsonic speeds and moderate-to-high angles of attack (flight conditions associated with takeoff and climb-out). The need for high-lift augmentation concepts is further accentuated by contemporary community noise standards and traffic congestion at Air Traffic Control stations. While there is ongoing research

---

<sup>+</sup> Senior Scientist

<sup>++</sup> Aerospace Engineer, Subsonic Aerodynamics Branch

<sup>+++</sup> Head, Subsonic Aerodynamics Branch

in this area at national research laboratories and private industry, (Brune and McMasters<sup>1</sup> provide an extensive review of computational high-lift design in practice at industry), a critical need exists for further innovations. For this to be realized, major breakthroughs in several areas must occur. From a computational perspective improved methods are needed to analyze geometrically complex systems and include key physics, such as flow separation, transition and turbulence, which dominate the flow fields. This paper attempts to review some of the issues which are crucial for computational fluid dynamics (CFD) to truly complement ground and flight based research and development for advanced high-lift systems.

Advanced transport designs currently receiving considerable attention include configurations designed for supersonic cruise, such as the High Speed Civil Transport (HSCT), as well as more conventional subsonic transports. High-lift systems for subsonic transports, typically use deflected leading edge slat surfaces and trailing edge slotted flaps for lift augmentation, see Figure 1. Figure 1a shows a relatively simple 3-component system consisting of a main element, slat and single slotted flap configuration which was tested by Lockheed-Georgia<sup>2</sup>. A more complex system shown in Figure 1b depicts a double slotted trailing-edge flap in addition to the slat and main element. This configuration was tested in the NASA Langley Low Turbulence Pressure Tunnel (LTPT)<sup>3</sup>. Subsonic high-lift systems, when fully deployed, can have regions of separation on the slat or flap, or in the cove regions. The subsonic systems may also have confluent boundary layers as a result of the strong interaction of shear layers. The subsonic high-lift systems are thus viscous dominated flow fields and have considerable geometrical complexity. Computational methods for high-lift systems must be carefully chosen to incorporate these varying requirements in flow

physics and geometry.

High-lift systems for supersonic configurations differ from those for subsonic transport systems both in system geometry and physics which dominate the flow. In order to achieve the desired high levels of supersonic cruise efficiency, many advanced supersonic configurations employ a low aspect ratio, highly swept wing. Unfortunately, these configurations typically have poor low-speed performance characteristics. Often, the low speed performance characteristics of these systems are enhanced either by attached flow or vortex flaps along the wing leading edge. Attached flow flaps are designed to suppress the formation of leading-edge vortices. Conversely, vortex flaps are designed to position the leading edge vortex within the bounds of the flap chord to provide a component of thrust which results from a vortex induced suction force. The trailing edge flap system for these configurations may consist of a segmented system of hinged flaps. Figure 2 shows the schematic of a low aspect ratio highly swept wing configuration tested at NASA<sup>4</sup>; the leading edge flap segments can be deflected independently about the hinge line. The trailing edge flap segments can also be deflected independently about the flap hinge lines. Also shown in Figure 2 are schematics of attached flow and vortex flap concepts. Grid systems to model these complex, segmented geometries must be highly versatile. In addition, the computational methods employed in the study of high-lift systems for supersonic configurations must be capable of capturing vortex structures with minimum smearing and phase distortion since the nature of the flow is highly vortical in these systems.

The problems of high-lift system analysis often include such issues as engine airframe integration and three-dimensional effects resulting from wing sweep, pylons, partial-span-flap deflections and tip ef-

fects. These attributes yield extremely complex geometries and attendant complex, interactional physical phenomena. While incremental progress by way of interactional methods or in development of quasi-three-dimensional analyses is being accomplished, we are not confident that such progress will computationally support innovative breakthroughs for future high-lift system design and development. Low cost, computationally efficient solutions (multi-grid, local time stepping) for three-dimensional steady flows for relatively simple geometries are available using thin-layer Navier-Stokes codes. We feel emphasis on these methods will yield substantial progress toward alleviation of the two major obstacles to accurate, efficient high-lift system analysis, viz., complex geometry and physics. Hence, our principal perspective will focus on Navier-Stokes solutions. In this paper, we explore some of the crucial issues which must be successfully addressed in order to develop computational methodology to analyze three-dimensional high-lift systems.

The following sections present a brief overview of experimental efforts useful for code calibration or validation along with a brief assessment of the computational state-of-the art. Geometric considerations are addressed within the context of the implications for grid generation. Issues related to code algorithms and dominant physics are briefly discussed for high-lift system applicability. Some of the salient efforts currently being pursued at NASA Langley are also presented. Concluding remarks consist of suggestions of major research areas where coordinated work is required to sustain progress for computational high-lift system analysis and design.

## II. Literature Overview

### Experimental database

While it is not the intent of this paper to review the available high-lift research literature, a brief overview of some salient reports is appropriate. Among the published data on multi-element airfoils, Braden, Whipkey, Jones and Lilley<sup>2</sup> report on a study of the confluent boundary layer development and separation characteristics on a NASA GAW-1. The section was equipped with a 29% chord single-slotted trailing edge flap and a 15% chord leading edge slat. Various combinations of slat and/or flap deflections and angle of attack were investigated in the study. The report contains surface pressure measurements on the airfoil as well as lift versus angle of attack curves for various flap/slat arrangements. Surface oil flows were used to provide flow visualization of boundary layer transition patterns. Boundary layer velocity profiles, turbulence intensities and Reynolds shear stresses for the configurations are reported under a separate cover<sup>5</sup>. A supplement to this report contains over 30000 sets of laser velocimetry (LV) derived boundary layer and wake data for the various combinations of geometric arrangements and angles of attack. In addition, off body flow field data were obtained using hot wire and LV.

Valerazo, Dominik, McGhee, Goodman and Paschal<sup>3</sup> have conducted multi-element airfoil optimization studies for maximum lift. This is a cooperative study between NASA and Douglas Aircraft Company. The primary focus of the study was to discern the high Reynolds number sensitivities of the multi-element airfoils at chord Reynolds numbers up to 16 million. The high-lift system consists of a double slotted flap and a single slotted slat as shown in Figure 2b. Among the data that are presented is the variation of  $C_{lmax}$  with Reynolds number, the variation of  $C_{lmax}$  with slat gap and the effect of flap

gap on  $C_{lmax}$ . No flow field surveys are reported from the study. In addition, there were no mechanisms used in the study for transition detection.

Olson and Orloff<sup>6</sup> report on the study of an airfoil with flap arrangement conducted in the NASA Ames Research Center 7 by 10 foot tunnel for Mach Number of 0.06 and a Reynolds number of 1.3 million. Surface pressure measurements, Reynolds stresses and detailed measurements of mean velocity in the boundary layers, wakes and merging layers are reported. The data should be considered purely incompressible and codes with compressible formulations will have difficulty in simulating this extremely low Mach number.

Wentz, Seetharam and Fisco<sup>7</sup> tested an aileron and a fowler flap applied to a GAW-1 airfoil. The experiment was conducted at  $M = 0.13$  and Reynolds number of 2.2 million. Aileron control effectiveness and hinge moments are presented for various gaps from 0 to 2% chord. For the fowler flap study, pressure distributions for various flap settings were obtained for a limited angle of attack range.

Adair and Horne<sup>8</sup> present pressure and velocity characteristics in the vicinity of the flap of a single slotted airfoil at a Mach number of 0.09 and a chord Reynolds Number of 1.8 million at the NASA Ames 7x10 foot tunnel. They report strong confluence effects on the boundary layer development on the flap suction surface due to the presence of a strong jet emanating from the slot flow. The flap is separation free except at the trailing edge where intermittent separation is observed. As a result of this the data may only be of limited use for steady state calculations. The flap wake development is reported to be asymmetric due to strong destabilizing curvature effects on the suction side. These data should therefore provide some guidance for studies of non-equilibrium effects on turbulence.

Morgan<sup>9</sup> and Morgan and Paulson<sup>10</sup> report on the study of static longitudinal and lateral directional aerodynamic characteristics of an advanced aspect ratio 10 and aspect ratio 12 supercritical wing transport model. The model was equipped with a high-lift system consisting of a full-span leading edge slat and partial-span and full-span trailing edge flaps. The Reynolds number of the tests varied from 0.97 to 1.63 million over a Mach number range of 0.12 to 0.20. The model was tested at angles of attack from -4 to 24 degrees and sideslip from -10 to 5 degrees. The model has engine nacelles, landing gear and movable horizontal tails. Six basic wing configurations were tested. These consisted of cruise (nested case), partial-span flap, full-span flap, full-span flap with low-speed ailerons and full-span flap with high-speed ailerons with slat and flap deflected to represent takeoff and landing conditions. Lift, drag and pitching moment data are presented for various cases.

Nakayama, Kreplin and Morgan<sup>11</sup> report detailed flow field measurements for a three-element airfoil with a conventional slat and single slotted flap. Reynolds stress distributions and mean flow measurements are presented on the main element and in the flap and wake regions. These suggest strong confluence effects in the flap region involving a jet-like stream from the flap-airfoil gap, the wake region of the main element with slat and the boundary layer on the flap itself.

The above cited works provides some data for code calibration or validation. However, there are large voids in the data base and measurements are not in sufficient detail to understand the complex flow physics that a computational study seeks to model. The flow in the gap region and pressure sides of many of these configurations needs to be documented

fully. There is also a need to obtain turbulent fluctuations data ( $u'$ ,  $v'$ ,  $u'v'$ ), transition location and mapping of flow confluence. Further studies in this area must be designed to closely follow the CFD needs to construct proper turbulence models and flow modules for Reynolds averaged Navier-Stokes calculations.

#### Computational database

Brune and McMasters<sup>1</sup> provide an excellent review of existing computational methods for analysis of high-lift systems. The status of these methods can be summarized as follows: there are presently no truly three-dimensional CFD methods for high-lift studies. Most three-dimensional studies use quasi-three-dimensional viscous approaches such as three-dimensional inviscid codes coupled with two-dimensional boundary layer codes. Existing viscous, two-dimensional airfoil codes can be classified, according to Ref.1, as, (I) Coupled Attached-Flow Methods, (II) Coupled Separated-Flow Methods, (III) Navier-Stokes Methods and (IV) Design and Optimization Methods. Categories (I), (II) and (IV) are widely used in industry today, while Category (III) is considered to be at the developmental stage. Both the attached and separated flow methods (Category (I) and (II)) are based on interactional boundary layer approaches while the Design and Optimization methods are clearly a patchwork of methods (I), (II) and simple inviscid analyses. In category (I), a boundary layer method is coupled to an inviscid flow calculation<sup>12,13,14</sup> and in (II), some form of modelling of the separated region is attempted<sup>15,16,17</sup>. The attached flow methods provide good agreement for lift at low angles of attack, where there is no flow separation. The separated flow models have been successful for some cases to compute maximum lift up to stall. These methods are at best useful in a limited fashion and do not promise to provide a successful methodology for high-lift system design. There

are also a few applications of two-dimensional Navier-Stokes solvers for high-lift configuration analysis in the literature. Schuster and Birckelbaw<sup>18</sup> and Shima<sup>19</sup> have obtained two-dimensional Navier-stokes solutions for multi-element airfoil systems using patched structured-grids. Using an unstructured-grid solver, Mavriplis and Martinelli<sup>20</sup> have also obtained solutions of two-dimensional multi-element airfoils. This work may well be a bellwether for high-lift system computations.

### III. Geometrical Considerations

Complex geometry issues associated with high-lift system analysis are non-trivial to say the least. Even when the problem is simplified to a wing with deflected surfaces (disregarding pylons, engines, flap track fairings, etc.), the task of surface modelling and field discretization is formidable. Geometries which are discontinuous in the streamwise and spanwise directions offer a significant challenge to the CFD community. Within these discontinuous regions flow interactions are occurring which can have significant and dominant effects on the resulting flow field. An example of this is the vortical flow occurring at the edge of a partial span leading-edge flap as it is deflected on a highly swept wing. The following sections address in some detail the manner in which CFD code developers are addressing these issues. From the structured grid perspective, single block, multi-block and Chimera schemes are each addressed. The promising work going on in the development of efficient unstructured grid generation techniques is also discussed. Finally, zonal methods are addressed including an example of their applications.

#### Structured-grid solvers

##### (a) Single and Multi-block methods

The rapid progress in CFD of the last

decade has made it possible to analyze simple wing-body geometries with relatively little effort. This is due, in part, to efficient grid generation techniques and acceleration techniques such as mesh sequencing, local time stepping and multi-grid techniques. Structured-grid algorithms, such as TLNS3D<sup>21,22,23</sup> and CFL3D<sup>24</sup>, have shown that for many steady flow problems, efficient solutions are possible using multigrid acceleration schemes. However, for the multi-element problems, the single block structured solvers are difficult to use. Fortunately, multi-block versions of these codes are currently being developed. These multi-block solvers may have the power to analyze complex domain problems by breaking the flow domain into smaller sub-domains or blocks of individual grid topology (such as grid system for each component of a multi-component system). The appropriate set of flow equations in each of these blocks can then be solved. Another significant development is the availability of powerful new grid generation packages which in the hands of experienced users can be used to do virtually any type of gridding (C-O; C-H; C-C) with relative ease. Among the most promising grid-generation packages are GRIDGEN<sup>25</sup> and EAGLE<sup>26</sup>. These are both user-friendly packages for generating two-dimensional and three-dimensional structured volume grids for finite volume analyses. Single or multi-blocked grids may be generated using these packages. The grid systems that may be constructed in the multi-blocks may or may not have  $C^0$  (common grid points) or  $C^1$  continuity (slope continuity as well as common grid locations) at the interface of these blocks. Depending on the nature of these interface conditions many variations of boundary coupling between various blocks are possible.

Previously, the utility of using structured-grid solvers for multi-element airfoil cases has been explored in the

context of two-dimensional flows. Using a structured-grid solver as the base code, Schuster and Birckelbaw<sup>18</sup> developed solutions for the multiple element airfoil problem by a multi-block approach using two-dimensional Navier-Stokes solutions. Figure 3 shows the schematic of the multiple-block grid topology used by them for a two-element airfoil. Figure 3a shows the arrangement of the various blocks in physical space and Figure 3b shows the arrangement in computational space. The line marked S is a line of singularity where all three blocks intersect and it requires special connectivity relations. The composite grid in Figure 3c is obtained by an iterative approach such that the grid systems in the regions retain  $C^0$  continuity at the block interfaces. The flow solver used in Ref.18 is a modified ADI scheme closely related to the Beam-Warming algorithm and the turbulence model used in the calculations is the Baldwin-Lomax model. Schuster and Brickelbaw obtain a reasonable comparison of  $C_l$  with experimental data at angles of attack up to stall as can be seen from the lift versus angle of attack curve shown in Figure 3d. They also state that their solution at the stall angle and beyond did not converge to a steady state solution. The curve shown by the dotted line in the figure is an average of the oscillatory solution. The  $C_p$  predictions on the main element obtained by them (not shown here) indicate some systematic variations from experimental measurements, the cause of which was unknown.

Shima<sup>19</sup> also obtained Navier-stokes solutions for a multi-element airfoil system using a patched grid system. The grid generation for the multiply connected domain in this work is again a non-trivial problem. Here, the composite grid is obtained in a two-step process. Initially, a potential flow solution around the multi-element airfoil is generated using a panel method. Next, conventional grid generation techniques<sup>27</sup>, using finite-dif-

ference methods, are employed where the computational co-ordinates are now the known potential and streamfunctions around the multi-element airfoil. This allows control of grid spacing required for the Navier-Stokes solutions near the body. The flow solver in Ref.19 uses an upwind (Total Variation Diminishing or TVD) scheme modified for low Mach number applications. Computed solutions are compared to experimental measurements of Foster, Irwin and Williams<sup>28</sup>. The results obtained for a two-element configuration (consisting of main element and flap) are shown in Figure 4 reproduced from Reference 19. The agreement between experimental data and computations for  $C_l$  is reasonable; the stall angle of attack predicted from the solution by the averaging method similar to that used in Reference 18 is under-predicted in the calculations. The authors postulate that this could be a result of numerical problems. The results for stall and post-stall cases are once again suspect since they are obtained by averaging an oscillatory solution obtained by the computer simulation.

While these results for two-dimensional cases suggest the utility of multi-block systems for high-lift analysis, further research is required to establish the usability of such methods for a highly complex three-dimensional configuration. For three-dimensional applications, the multi-block methods with rule based expert systems may provide a natural way for generating structured grids for analysis. Dannenhoffer<sup>29</sup> discusses the development of such a system for two-dimensional multi-body configurations. With elements in close proximity, the nature and quality of such grids and their resultant sensitivity to overall flow solution need to be examined closely. Many of the finite volume structured solvers are highly sensitive to grid quality. The inability of these methods to provide reasonable simulations in regions where the grid may be highly distorted and stretched, such as,

in the narrow regions of flow passage around the multi-element airfoil case, may limit the use of these methods for 3D-high-lift analysis. The complexity of the grid-generation and flow solver may also have some bearing on their eventual acceptance.

#### (b) Overlapping Grids/Chimera Schemes

In addition to the multi-block method, grid overlapping methods are another commonly used technique for domain decomposition. In overlapping schemes the sub-domains and the grid systems associated with them may overlap, or it may be possible to embed one sub-domain completely in another. In the "chimera scheme"<sup>30</sup>, the regions of a grid common to others is removed thereby creating voids or holes inside the grid. Baysal et. al.<sup>31</sup>, have looked at the quality of chimera solutions by studying the solutions with and without embedding for a test problem and conclude that there are only "minor" differences between the solutions. If this is true, chimera schemes may offer the flexibility to study multi-element airfoil flows. An example of a chimera grid developed at NASA Langley Subsonic Aerodynamics Branch for the GAW-1 airfoil with a deployed slat is shown in Figure 5. Figure 5a is an example of a sub-domain which consists of the slat geometry. Each sub-domain (see, Figure 5a,b) contains a "hole" or void in it which is a region of overlap of another sub-domain. The void is identified for each sub-domain in a preprocessing step. The solution strategy for the composite flow field involves computation of flow fields in each sub-domain with the associated boundary values including those for the boundaries of the void region. Since the boundary values for the voids are generated iteratively (by solutions from the sub-domains that create the voids), convergence of these methods depends strongly on how well the boundary values are approximated.

Figure 6 shows Euler solutions obtained by Biedron<sup>32</sup> using CFL3D employing an overlapped grid option for an airfoil with a slat. The calculated conditions are at  $M=0.5$  and  $\alpha = 7.5^\circ$ . These excellent results suggest that the overlapped grid option may be exploited to generate grid structures over multi-component airfoils.

An important advantage of the chimera scheme or the overlapped grid methods is the relative ease with which structured-grids can be generated around "simple" sub-domains of a complex three-dimensional domain. Buning, Parks, Chan and Renze<sup>33</sup> describe the application of a chimera scheme for the space shuttle ascent geometry. The component grids were generated using a hyperbolic grid generation technique which is faster than elliptical grid generators. Due to the complexity of the geometry, the grid joining process does become somewhat involved at the intersection of geometrical components. Further innovation in the form of "collar grids"<sup>34</sup> were required to develop solutions for the shuttle ascent geometry. An example of a "collar grid" for a cylinder intersecting a curved surface is shown in Figure 7 (reproduced from Ref.34). Figure 7a shows the combined collar surface grid. The white region in the figure is the void in the cylinder and the plane surfaces. The collar grid separates the intersecting surfaces and acts as a transitional zone between them. Figure 7b shows a slice of the collar grid and the chimera grids around it.

The overlapping schemes and in particular, the chimera scheme provide a simple way to generate computational grids. However, further study is required to sort out any sources of error in such an approach before recommending these methods as a panacea for high-lift system analyses. Buning et.al.<sup>33</sup> point out that while the accuracy of their solutions improved with improved modelling of the geo-

metry, the accuracy required for wing loading analyses is significantly higher than obtainable with chimera schemes. Effective use of chimera is also limited, according to them, by difficulties for the scheme in implementing turbulence models based on length scales for multi-body configurations.

### Unstructured-grid methods

Navier-Stokes solvers using unstructured-grids (triangular, tetrahedral meshes) are relative newcomers to the field. While finite element methods using triangular and quadrilateral and tetrahedral elements have been used in the past, their applications have been limited to low Reynolds number flows. Mavriplis<sup>35</sup>, Mavriplis and Martinelli<sup>20</sup> and Mavriplis and Jameson<sup>36</sup> have led the way in developing viable solutions to flow over airfoils. The implementation of multigrid strategy and turbulence modelling for the two-dimensional cases are major assets to the flow solver used in Reference 20. At present several multi-component flows have been calculated using this version of the code and good agreement with experimental data has been obtained for many of these cases. For example, Reference 20 documents solutions of multi-element airfoils which show excellent agreement with experimental data using a two-equation ( $k-\epsilon$ ) model.

The advantage of using unstructured-grids for analyzing high-lift systems is obvious. They are capable of properly modelling all the geometric complexity associated with high-lift systems in a straightforward manner. Figure 8 shows an unstructured-grid system developed at Subsonic Aerodynamics Branch (SAB), NASA Langley Research Center, for the study of a fully deployed low speed multi-element airfoil. An important merit of these methods is the ease and ability to adapt to an evolving solution. By using Delaunay triangulation techniques, the re-gridding in the region of interest can be

carried out in  $O(N^{3/2})$  operations for 2-D applications and in  $O(N^{5/2})$  operations for 3-D applications.

While the unstructured-grid techniques offer ease of grid generation and grid adaptation, the solvers used in these methods do not appear as computationally efficient as the structured-grid solvers. Indeed, comparisons have found them slower by a factor of 3 to 4 for many test cases<sup>37</sup> (the estimate given is for a 2-D code here; the estimate for 3-D viscous flows is much worse for the same accuracy; see for example the timings given in Ref. 21 for viscous calculations). The relative merit of such comparisons is somewhat suspect, since these test problems have no geometrical complexity and thus belong naturally in the domain of structured-grid solvers. The unstructured-grid methods do provide the power to analyze complex flow problems that are difficult to analyze using structured-grid solvers. Thus the development of unstructured-grid technology is receiving considerable attention and is progressing rapidly at various laboratories.

However, many major hurdles remain to be overcome before we have available a good three-dimensional unstructured-grid solver for viscous flows. The most significant of these hurdles is related to the directional sensitivity of the viscous flows. While the triangulation or tetrahedral domain discretization does not have a preferred orientation, flows with boundary layers do have directional sensitivity (i.e., boundary layers grow normal to the surface). Hence, some directivity needs to be introduced into the grid generation (non-Delaunay and hence more time consuming) and solution algorithms (background grids for turbulence, generation of many levels of grid for multi-grid implementations, etc.). Thus, while the Euler solver implementation is rather straightforward for the unstructured meshes, the implementation for high

Reynold number viscous flows offers a significant challenge. At present, this complexity seems to be the stumbling block in extending these methods to three-dimensional viscous flow problems. Obviously, new development in this area needs to occur.

### Zonal Methods

In zonal methods, the computational domain is divided into sub-domains where grids are patched together. A discriminating feature of these techniques relative to multi-block or chimera schemes is that the sub-domains may have varying degrees of latitude in the modelled physics. Normally, the zonal boundaries will be two-dimensional surfaces and they will have to be regular. The zonal approach offers the ability to properly model the physics through solution approximation valid to particular zones. For example, a fully elliptic flow problem may be solved using a zonal method where the flow regime may be approximated by a parabolic system of equations in a large zone and by the full elliptic system in a smaller zone. Depending on the size of these domains a large savings in computational resources may occur. Sankar, Bharadvaj and Tsung<sup>38</sup> use a zonal approach employing a full Navier-Stokes solution zone embedded in an outer potential flow field to study an F5 wing and an isolated helicopter rotor in hover. They show a savings of roughly 50% in computational time over full Navier-Stokes solutions for similar accuracy.

From the perspective of high-lift system studies, zonal approaches offer possibilities that are yet to be fully explored. Using zonal approaches, it may be possible to couple structured-grids with unstructured meshes to develop a flexible approach to three-dimensional problems. Another application of this technique may be in the analysis of separated flows, where the thin-layer approximations may break down and a full Navier-Stokes solu-

tion may be required in some zones of the flow field. Such an approach has the potential for generating a computationally efficient and accurate prediction method.

#### IV. Algorithmic Issues

##### Differencing schemes

There are several issues related to algorithms for high-lift studies that need to be examined. Upwind schemes which perform very well for supersonic flows have been known to perform rather poorly for low subsonic flows<sup>39</sup>. Central difference schemes, which work well for subsonic flows do depend to a degree on carefully tuned artificial dissipation to stabilize calculations (blended second and fourth order dissipations, residual smoothing, etc.). However, for subsonic flow calculations the central differencing algorithm is probably the most well behaved. The accuracy of these two schemes should be studied on prototype problems by systematic application. Based on the outcome it may turn out that one particular solution algorithm is more suitable than the other for a given configurational analysis. An unstructured-grid algorithm, for example Mavriplis<sup>36</sup>, which uses central differencing schemes may be more suitable for subsonic configuration studies, while other unstructured-grid solvers such as that by Batina<sup>40</sup> and Frink<sup>41</sup> which use upwind-based schemes may be more suited for vortical flows. It is possible that no single scheme (central difference / upwind scheme) will be appropriate for all cases. For example, consider the low aspect ratio, highly swept wing case. Here an upwind based scheme with controlled dissipation (e.g., TVD schemes) should predict the formation of vortices and their evolution in space more accurately than the central difference method where some smearing of the vorticity may occur due to added dissipation in most models.

For unstructured-grid solvers, there are other issues related to their speed and accuracy that need to be fully explored, such as, whether vertex based or cell centered schemes are the most appropriate for the solver. The formal accuracy of these methods depends to a large degree on the particular reconstruction method chosen. Cell vertex schemes are more economical for three-dimensional (tetrahedral elements) unstructured grids<sup>42</sup>, while cell centered schemes are more robust compared to cell vertex schemes<sup>43</sup>. Efficient cell-centered schemes for three-dimensional problems are possible with tetrahedral elements as demonstrated by Frink<sup>41</sup>. There are also approaches which combine vertex based schemes with cell-centered approach for integration of fluxes (see Reference 43). The computational efficiency and accuracy of these approaches must also be examined in detail. Lomax<sup>44</sup> suggests that there needs to be a further examination of special forms of structured grids in 2D and 3D to serve as a means for understanding and evaluating unstructured grid solvers and their formal accuracies.

While many of these issues will be considered by code developers, the applied scientist working on high-lift system studies will probably be involved in developing methods and grids that will support solving flow fields around configurations with considerable geometrical complexities. It is quite conceivable that the most useful approach might be one that incorporates hybrid techniques. An example of this approach is a multi-zonal scheme employing hybrid computational algorithms, grid structures and/or flow equation models for the high-lift system configurations.

##### Flow physics

Progress in computational methods for high-lift systems strongly depends on the ability to model turbulence, and predict transition, flow separation and reattach-

ment. For subsonic transport systems, in deployed high-lift situations, there may be cove, leading-edge slat, trailing-edge flap or main element flow separation. In some of these cases, the separated flow may be a massive shear layer which interacts with a boundary layer developing on an element downstream. The current state of the art in CFD does not address massively separated flows adequately. This deficiency leaves CFD yielding rather impotent analyses for high-lift systems as a result of the inability to predict where the flow begins to break down.

There are also other important flow physics which CFD is at present unable to address. For example scale effects for high-lift systems do not show a consistent pattern<sup>45</sup>. These anomalies are difficult to simulate computationally as a result of the significant computational resources required to compute flow conditions at flight Reynolds numbers. Relaminarization is a phenomenon which often occurs on the main element of a high-lift system in the influence of a deployed slat. This results as the flow on the main element accelerates around the leading edge due to extremely favorable pressure gradients at high Reynolds numbers<sup>46</sup>. Viscous wake interactions is another area requiring further insightful studies.

There are also areas that require immediate attention from a computational viewpoint. For example, the status of turbulence modelling for aerodynamic flows is rather primitive. There are two types of problems to be addressed here. One involves a limited understanding of transitional flows and boundary layers and the other is the inability to properly model turbulence. As a result of the inability to predict transition, calculations are often run in full "laminar" or "turbulent" options for many code comparisons. However, most experimental data are obtained for mixed laminar/turbulent flow fields. Some codes such as TLNS3D can be

run in the tripped mode. That is, if the location of transition from the laminar to turbulent state is known, the code will be able to compute non-zero eddy viscosity in the turbulent region. Even this approach is inherently deficient since the initial evolution of turbulence (low turbulent Reynolds numbers,  $R_T < 500$ ) is not properly modeled by existing turbulence models. An improved understanding of transitional boundary layers and transitional zonal modelling is clearly needed. Narasimha<sup>47</sup> advocates using a semi-empirical approach to the problem.

The other problem relates to the actual turbulence modelling itself. Menter<sup>48</sup> evaluated the performance of four popular turbulence closure models for flows under adverse pressure gradients. The Baldwin-Lomax, Johnson-King, Baldwin-Barth and Wilcox's  $k-\omega$  models were implemented in an incompressible Reynolds-averaged Navier-Stokes solver (INS code). Menter concluded that "the three non-equilibrium models gave significantly better results than the algebraic Baldwin-Lomax model" under strong adverse pressure gradients. Conclusions, which are not discussed here, were also presented relative to the performance of the three models. The authors feel that similar rigorous studies are crucial to understand the performance of these and other proposed turbulence models for multi-component airfoils and wings.

In addition, we feel for multi-element airfoil and wing problems, turbulence models based on length scales are more likely to fail since the choice of the appropriate length scale is difficult to identify. Complex turbulence models which do not depend on length scales may be the only answer. Even after solving the length scale problem, experience with many higher moment methods has been that their performance may not be that attractive considering the additional complexities they introduce, see the discussion by Lumley<sup>49</sup> as well as the comparison of various

turbulence models conducted in the AFOSR-Stanford Turbulence Meeting<sup>50</sup>.

However, there are some promising new developments in turbulence modelling, such as, second-order closure<sup>51</sup> and the Re-Normalized Group (RNG) based models<sup>52</sup>, that have appeared over the horizon. Results obtained using RNG methods are compared in Figure 9 (reproduced here from Reference 52) with those using Baldwin-Lomax model for the RAE2822 airfoil case. Figure 9a presents the results obtained using RNG model and Figure 9b presents results obtained using Baldwin-Lomax model. Note that the RNG solutions improve the prediction of the shock structure relative to the Baldwin-Lomax model both in shock location and strength. This model has undergone further developments since that time and appears to be ready for application to two and three-dimensional solvers of multi-component configurations. For example, a modified RNG k- $\epsilon$  formulation<sup>53</sup> has been shown to produce excellent agreement for the classical backward-facing step problem which all of the other turbulence models in use have difficulty in predicting (see Reference 50 and the discussions pertaining to the backward facing step pp 275-283; pp 886-911). A notable feature of the RNG formulation is that the model constants are not ad hoc and are derived by a consistent perturbation analysis of the Renormalised Navier-Stokes equations. These models may provide an avenue to improve the prediction for high angle of attack problems where the effects of turbulence are much more pronounced. As more and more reliance is placed in optimizing configurations for maximum lift to drag ratios or minimum drag, we will be forced to examine in detail the agreement that these Navier-Stokes codes provide for integral quantities.

#### V. Ongoing work

The high-lift elements of NASA's High

Speed Research (HSR) and Advanced Subsonic Transport Program have provided the impetus for several significant high-lift efforts at Langley Research Center. The elements consist of a balanced experimental and computational research program. Experimental work supporting the HSR Program involves testing a series of configurations with different types of leading-edge high-lift devices (attached flow and vortex flaps) and planform variations (different leading edge sweeps and aspect ratios). Data obtained in these tests include force and moment, surface pressure and flow visualization. A complementary computational program is being pursued to study the grid generation tools and computational methods required to analyze this class of vehicle. Due to the complexity of modelling the three dimensional high-lift system, the initial CFD effort concentrated on gridding and analyzing geometries with undeflected leading-edge devices. Once the cruise geometry is successfully analyzed the next step will be to analyze the high-lift configuration. Figure 10a is an example of an HSCT concept that was designed for a cruise Mach number of 3.0. This design consists of a blended wing body with a flattened or "platypus" forebody. The configuration was analyzed by Victor Lessard of Vigyan with the multi-block version of CFL3D<sup>24</sup> (a thin layer, upwind N-S code). Figure 10b shows a comparison of the surface pressure distributions obtained computationally with results obtained in the 8-foot Transonic Pressure Tunnel at NASA Langley. The comparisons shown are for two cross sections on the configuration. The first is near the nose and the second is just upstream of the wing crank. Both comparisons show excellent agreement between the computations and experiment. The pressure peaks indicative of vortex flow are well captured by the analysis. Due to the agreement between theory and experiment obtained on this and other cruise geometries, we feel the method will prove useful for analyzing simple three-

dimensional high-lift systems such as full-span attached flow flaps.

Another CFD effort that is being pursued by Kevin Kjerstad of NASA Langley in support of the HSR Program includes evaluation of the three-dimensional unstructured grid generator and Euler code developed by Frink, et al<sup>41</sup>. The grid generation method is based on the "advancing front technique" and uses a structured background grid to ease implementation of the grid generation process. An example of an unstructured grid generated for a generic high speed research configuration is shown in Figure 11a. The Euler solver, known as USM3D, is an upwind scheme developed for solving the three-dimensional Euler equations on unstructured tetrahedral meshes. The code uses a cell-centered, finite-volume formulation with flux-difference splitting for spatial discretization. Experimental and USM3D results on the generic configuration at subsonic speeds for lift, drag and pitching moment are compared in Figure 11b. Since the model has a sharp leading edge, the point of separation for the primary vortex is well defined and the Euler results should be reasonable. The comparisons in Figure 11b show excellent agreement between theory and experiment for all three quantities at the three angles of attack analyzed. The next step is to use the codes to analyze a three-dimensional high-lift system. The vortex flap concept is a good candidate for analysis since it has a sharp leading edge, hence, the separation point is known a priori. This configuration will be analyzed in the near future.

One of the efforts supporting the Advanced Subsonic Transport Program at NASA Langley involves assessing the capability of various computational techniques for high-lift system application. We are currently involved in assessing the capability of a structured-grid solver (TLNS3D) to predict the subsonic characteristics of a standard low-speed airfoil (GAW-1) at

angles of attack up to  $C_{lmax}$ . This solver is a transonic code with a central differencing scheme, that can be run with either the Baldwin-Lomax or the Johnson-King turbulence model. Experimental data for a GAW-1 airfoil obtained by McGhee and Beasley<sup>54</sup> has been chosen for computational studies. This particular airfoil has geometrical characteristics (thick airfoil section with blunt trailing edge) which can pose problems for a grid sensitive algorithm. Tests were conducted between Mach numbers of 0.10 to 0.28 and angles of attack from  $-10^\circ$  to  $24^\circ$ . The low Mach number data at  $M=0.15$  has been chosen by us to study the robustness of the transonic structured-grid code. For the experiments, transition was fixed at 8% chord and the solver has the capability to compute laminar calculations up to this location and thereafter, switch to a turbulent calculation. The results presented below are only for the Baldwin-Lomax model since the performance of the Johnson-King model was affected by grid quality for this particular geometry. Figure 12 shows the  $C_p$  comparison between experimental measurements and computation using the Baldwin-Lomax turbulence model in TLNS3D. Computations employing the Johnson-King model were adversely affected by grid quality for this particular geometry and are not presented here. The agreement between the computed solution and experimental data is extremely favorable up to  $8^\circ$  angle of attack. Beginning at  $12^\circ$ , the computed pressure distributions show differences with experimental data at the trailing edge region. These differences become progressively worse at higher angles of attack. At  $12^\circ$  and beyond, it was noted by the experimenters that there was trailing edge flow separation which became progressively larger with angle of attack. The computed wall shear stress data as well as Mach contour plots (not shown here) do indicate trailing edge flow separation at  $12^\circ$  which becomes progressively worse at higher angles of attack. The degree and extent of agreement between

experiment and theory in this separated zone is suspect since the included physics is deficient e.g, thin-layer approximation which breaks down in the vicinity of separation point (no streamwise viscous stress variation) and the turbulence model (Baldwin-Lomax model) used. The comparison of sectional lift versus angle of attack (Figure 13) shows that the lift is predicted rather well by the code up to an angle of attack of  $18^\circ$ , indicating that sectional lift is insensitive to the minor differences in pressure distribution observed. The drag comparison (Figure 14) shows the predictions are only accurate up to an angle of attack of  $8^\circ$ . Obviously, minor differences that are observed in pressure distributions have a larger influence on  $C_d$  than  $C_l$ . Since, lift to drag ratio issues may dominate future system designs, the challenge to code validators is obvious.

Bonhaus, Anderson and Mavriplis<sup>55</sup> are using the unstructured-grid solver of Mavriplis to analyze multi-component airfoils for subsonic transport applications. The experimental data used in this comparison is from a Douglas four element configuration tested at the Langley LTPT tunnel. The computed pressure distribution over the elements have been compared against experimental data for angles of attack of 0, 12, 18 and 20 degrees. These results were obtained using the Baldwin-Lomax turbulence model. The agreement between experimental data and computations are extremely good up to  $C_{l_{max}}$ . At 0 degree angle of attack, (not shown here), the biggest difficulty is in predicting the slat pressure distribution in the cove region. At higher angles of attack, the computed results agree very well with measurements on the slat surface, while the prediction is off from experiment in the auxiliary flap as can be seen from Figure 15a. At 20 degree angle of attack, Figure 15b, the disagreement is quite pronounced for both the main and aft flap indicating the wake viscous interactions are not fully cap-

tured by the code. Figure 16 shows the lift vs angle of attack curve. Again, the predictions are in good agreement with experiment up to  $C_{l_{max}}$ . Beyond  $C_{l_{max}}$ , the computed lift curve shows an increase in lift with angle of attack, demonstrating the inability of the method to predict stall behavior.

Previously in this paper discussions and examples of grids for multi-element airfoils have been presented. As has been stated, the gridding and analysis of a three-dimensional high-lift system is quite difficult. The grid generator and Euler code described above (Reference 41) were used by Dr. Mohammad Takallu of Lockheed and Dr. Simha Dodbele of Vigyan to study a multi-element wing. The wing chosen was a unswept, semi-span wing consisting of a main element and full-span, double slotted flap. The surface grid on the configuration and part of the symmetry plane mesh is shown in Figure 17. Even though this geometry is complex, the grid generation process was relatively straight forward. As data become available, the results of the Euler analysis will be evaluated to determine the utility of the code for high-lift configuration analysis for attached flow conditions.

Another difficulty with high-lift system design and analysis is the proximity of the ground and the effect this has on the flow field surrounding the configuration. Often there is a significant effect on lift due to the interference of the wing flow field and the ground. Figure 18 is an example of an unstructured grid developed by Kyle Anderson of NASA Langley for a multi-component airfoil in ground effect. The airfoil is placed in the proper orientation above the ground and then the grid is generated using Delaunay triangulation techniques. The ground is simulated by adding a zero transpiration boundary condition to the boundary below the airfoil. To analyze other ground heights for this same airfoils, the grid

must then be regenerated with the airfoil placed in its new position. Due to the adaptability of unstructured grid generation techniques, this requires relatively little input by the researcher.

Ground effect analysis can also be done using a structured grid approach. Fig. 19 is an example of a structured grid generated by Dr. Steve Yaros of Langley for a National Aerospace Plane (NASP) type configuration in close proximity to the ground. In this case the analysis was done using a Navier-Stokes code; so a no slip boundary condition was imposed at the wall. Again, to analyze the configuration at different ground heights requires regeneration of the grid. For this simple geometry in Figure 19 the process is straightforward. However, for more complex configurations, generating new multi-block grids could be time consuming.

#### VI. Future Plans

Based on the discussions above it is possible to identify several areas where further coordinated work is needed.

(i) Generation of a data base that can be used for developing models of flow physics for computer simulation. This requires the generation of detailed L-V data, shear stress, energy and fluctuation measurements. These measurements pose a significant challenge for multi-component airfoils where there are narrow regions of flow. A systematic effort should also be made to compare computed solutions using heuristic models with existing data bases.

(ii) Further research is necessary to develop three-dimensional structured and unstructured-grid generation techniques and development of hybrid (zonal) methods for viscous flows. Intelligent use of an expert system may allow development of efficient three-dimensional blocked grids for geometrically complex configurations.

(iii) A concerted effort should be made to develop new turbulence models for separated flows and to test these models in flow codes. There are few and relatively poor performing turbulence models for separated flows currently available. Progress made in this field is bound to provide rich rewards. There are currently several good candidates such as the model of Wilcox<sup>56</sup>, RNG models, and second order closure models, that need to be validated.

(iv) The need for co-ordinated efforts between industry and government laboratories needs to be addressed. With such vast areas of research to be done, a collaborative industrial-government consortium would serve to reduce duplication of data and effort at this critical juncture.

#### References

1. Brune, .W. and McMasters, J.H., "Computational Aerodynamics Applied to High-lift systems," In Applied Computational Aerodynamics, pp. 389-433, AIAA, 1990.
2. Braden, J. A., Whipkey, R. R., Jones, G. S. and Lilley, D. E., "Experimental Study of the Separating Confluent Boundary-Layer Volume I- Summary," NASA CR-3655, 1983.
3. Valarezo, W. O., Dominik, C. J., McGhee, R. J., Goodman, W. L. and Paschal, K. B., "Multi-Element Airfoil Optimization for Maximum Lift at High Reynolds Numbers," AIAA Paper 91-3332, September 1991.
4. Coe, P. L. and Weston, R. P., "Effects of Wing Leading-Edge Deflection on Low-Speed Aerodynamic Characteristics of a Low-Aspect-Ratio Highly Swept Arrow-Wing Configuration," NASA TP 1434, 1979.
5. Braden, J.A., Whipkey, R.R., Jones, G.S. and Lilley, D.E., "Experimental Study of the Separating Confluent Boundary-Layer Volume II - Experimental Data," NASA CR 166018, March 1983.
6. Olson, L.E. and Orlof, K. L., "On the Structure of Turbulent Wakes and Merging Layers of Multi-Element Airfoils," AIAA Paper 81-1248, June 1981.

7. Wentz, W. H. Jr., Seetharam, H. C. and Fisco, K.A., "Force and Pressure Tests of the GA(W)-1 Airfoil with a 20% Aileron and Pressure Tests with a 30% Fowler Flap," NASA CR-2833, June 1977.
8. Adair, D. and Horne, W. C., "Turbulent Separated Flow in the Vicinity of a Single Slotted Airfoil Flap," AIAA Paper 88-0613, January 1988.
9. Morgan, H. L., Jr., "Low-Speed Aerodynamic Performance of an Aspect-Ratio-10 Supercritical Wing Transport Model Equipped with a Full-Span Slat and Part-Span and Full-Span Double-Slotted Flaps," NASA TP 1805, April 1981.
10. Morgan, H. L. Jr. and Paulson, J.W., "Low-Speed Aerodynamic Performance of a High-Aspect Ratio Supercritical-Wing Transport Model Equipped with Full-Span Slat and Part-Span Double Slotted Flaps," NASA TP 1580, 1979.
11. Nakayama, A., Kreplin, H.P. and Morgan, H.L., "Experimental Investigation of Flowfield About a Multi-Element Airfoil," AIAA Journal, January 1990.
12. Stevens, W. A., Goradia, S.H. and Braden, J.A., "Mathematical Model for Two-Dimensional Multi-Component Airfoils in Viscous Flows," NASA CR1843, July 1971.
13. Morgan, H. L., Jr., "A Computer Program for the Analysis of Multi-Element Airfoils in Two-Dimensional Subsonic, Viscous Flows," NASA SP-347, March 1975.
14. Dvorak, F.A., and Woodward, F.A., "A Viscous/Potential Flow Interaction Analysis Method for Multi-Element Swept Wings," NASA CR-2476, November 1974.
15. Mani, K. K., "A Multiple Separation Model for Multi-Element Airfoils," AIAA Paper 83-1844, July 1983.
16. King, D.A., and Williams, B.R., "Developments in Computational Methods for High-Lift Aerodynamics," Aeronautical Journal, Vol. 92, No. 917, 1988, pp 265-288.
17. Cebeci, T., Chang, K.C., Clark, R.W. and Halsey, N.D., "Calculation of Flow over Multi-Element Airfoils at High Lift," Journal Of Aircraft, Vol. 24, No.8, 1988.
18. Schuster, D.M. and Brickelbaw, L.D., "Numerical Computation of Viscous Flowfields about Multiple Component Airfoils," AIAA Paper 85-0167, January 1985.
19. Shima, E., "Numerical Analysis of Multiple Element High Lift Devices by Navier Stokes Equation using Implicit TVD Finite Volume Method," AIAA Paper 88-2574-CP, June 1988.
20. Mavriplis, D.J., and Martinelli, L., "Multigrid Solution of Compressible Turbulent Flows on Unstructured Meshes Using a Two-Equation Model," AIAA Paper 91-0237, January 1991.
21. Vatsa, V.N. and Wedan, B.W., "Development of a Multigrid Code for 3-D Navier-Stokes Equations and its Application to a Grid Refinement Study," Computers and Fluids, Vol. 18, No.4, 1990.
22. Vatsa, V. N., "Accurate Numerical Solutions for Transonic Viscous Flows over Finite Wings," Journal Of Aircraft, Vol. 24, No. 6, 1987.
23. Vatsa, V.N., Turkel, E., and Abolhasani, J.S., "Extension of Multigrid Methodology to Supersonic/Hypersonic 3-D Viscous Flows," Fifth Copper Mountain Conference on Multigrid Methods, 1991.
24. Thomas, J.L., Krist, S.T., and Anderson, W. K., "Navier-Stokes Computations of Vortical Flows Over Low Aspect Ratio Wings," AIAA Journal, Vol.28, No.2, 1990.
25. Steinbrenner, J.P., Chawner, J.R., and Fouts, C.L., "The GRIDGEN 3D Multiple Block Grid Generation System, Volume I: Final Report," WRDC-TR-90-3022.
26. Thompson, J.F., "Project EAGLE -Numerical Grid Generation System User's Manual, Vol.3: Grid Generation Code," USAF Armament Laboratory Technical Report, AFATL-TR-87-15, 1987.
27. Thompson, J.F., Thames, F.C. and Mastin, C.W. "TOMCAT- A Code for Numerical Generation of Boundary Fitted Curvilinear Coordinates on Field Containing Any Number of Two-Dimensional Bodies," J. Comp.Phys., Vol.24, 1977.
28. Foster, D. N., Irwin, H.P.A., and Williams, B.R., "The Two-Dimensional Flow Around a Slotted Flap," ARC Report and Memoranda No. 3681, 1970.
29. Dannenhoffer, J. F., III, "Computer-Aid-

- ed Block Structuring Through the Use of Optimization and Expert System Techniques," AIAA Paper 91-1589-CP, Honolulu, June 1991.
30. Steger, J.L., Dougherty, F.C. and Benek, J.A., "A Chimera Grid Scheme," Advances in Grid Generation, ASME, New York, FED-Vol.5, June 1983.
31. Baysal, O., Fouladi, K., and Lessard, V. R., "Multigrid and Upwind Viscous Flow Solver on Three-Dimensional Overlapped and Embedded Grids," AIAA Journal, Vol.29, No. 6, 1991.
32. Biedron, A. S & M Inc., Private Communications.
33. Buning, P. G., Parks, S. J., Chan, W. M. and Renze, K.J., "Application of the Chimera Overlapped Grid Scheme to Simulation of Space Shuttle Ascent Flows," Proceedings of the Fourth International Symposium on Computational Fluid Dynamics, Vol I, pp.132-137, Sept. 1991.
34. Parks, S. J., Buning, P. G., Steger, J.L. and Chan, W.M., "Collar Grids for Intersecting Geometrical Components Within the Chimera Overlapped Grid Scheme," AIAA Paper No. 91-1567-CP, Honolulu, June 1991.
35. Mavriplis, D.J., "Multigrid Solution of the 2-D Euler Equations on Unstructured Triangular Meshes," AIAA Journal, Vol.26, July 1988.
36. Mavriplis, D. J. and Jameson, A., "Solution Of the Navier-Stokes Equations on Triangular Meshes," AIAA Journal, vol. 28, No. 8, 1990.
37. Mavriplis, D.J., "Accurate Multigrid Solution of the Euler Equations On Unstructured and Adaptive Meshes," NASA CR-181786, February 1989.
38. Sankar, L.N., Bharadwaj, B.K. and Tsung, Fu-Lin, "A Three-Dimensional Navier-Stokes/Full Potential Coupled Analysis for Viscous Transonic Flow," AIAA Paper No. 91-1595-CP, Honolulu, June 1991.
39. Hanel, D., Schwane, R. and Seider, G., "On the Accuracy of Upwind Schemes for the Solution of the Navier-Stokes Equations," AIAA Paper 87-1105, January 1987.
40. Batina, J.T., "Accuracy of an Unstructured-Grid Upwind-Euler Algorithm for the Onera Wing," Presented at Accuracy Of Unstructured Grid Techniques Workshop, NASA LaRC, January 1990.
41. Frink, N.T., Parikh, P. and Pirzadeh, S., "A Fast Upwind Solver for the Euler Equations on Three-Dimensional Unstructured Meshes," AIAA Paper No. 91-0102, January 1991.
42. Barth, T. J., "A 3-D Upwind Euler Solver for Unstructured Meshes," AIAA Paper No. 91-1548-CP, Honolulu, June 1991.
43. Hall, M. G., "A Vertex -Centroid Scheme for Improved Finite- Volume Solution of the Navier-Stokes Equations," AIAA Paper No. 91-1540-CP, Honolulu, June 1991.
44. Lomax, H., "CFD in the 1980'S from One Point of View," AIAA Paper No. 91-1526-CP, Honolulu, June 1991.
45. Woodward, D.S. , Hardy B.C. and Ashill, P. R., "Some Type of Scale Effects in Low-Speed High-Lift Flows," ICAS Paper 4.9.3, Jerusalem, 1988.
46. Garner, P. L., Meridith, P.T. and Stoner, R.C., "Areas for Future CFD Development as Illustrated by Transport Aircraft Applications," AIAA Paper No. 91-1527-CP, Honolulu, June 1991.
47. Narasimha, R., "Modelling the Transitional Boundary Layer", NASA CR-187487, 1990.
48. Menter, F.R., "Performance of Popular Turbulence Models for Attached and Separated Adverse Pressure Gradient Flows," AIAA Paper No. 91-1784-CP, Honolulu, June 1991.
49. Lumley, J.L., "Turbulence Modeling," J. App. Mechanics, Vol.50, No.12, 1983, pp.1-097-1103.
50. Kline, S.J., Cantwell, B.J. and Lilley, G.M., "The 1980-81 AFOSR-HTTM-Stanford Conference on Complex Turbulent flows: Comparison of Computations and Experiment I, II, and III," Thermosciences Division, Mechanical Engineering Department, Stanford University, Stanford, Calif., 1981.
51. Sarkar, S and Speziale, C. G., "A Simple Nonlinear Model for the Return to Isotropy in Turbulence," Phys. Fluids A, Vol. 2, No.1, January 1990.
52. Martinelli, L. and Yakhot, V., "RNG-Based Turbulence Transport Approximations

with Applications to Transonic Flows," AIAA Paper 89-1950, June 1989.

53. Yakhov, V., Thangam, S., Gatski, T. B., Orszag, S.A. and Speziale, C.G., "Development of Turbulence Models for Shear Flows by a Double Expansion Technique," NASA CR-187611, July, 1991.

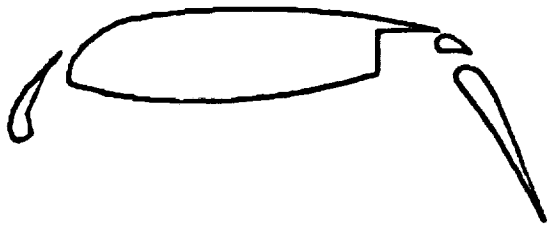
54. McGhee, R. J., and Beasley, W. D., "Low-Speed Aerodynamic Characteristics of a 17-Percent-Thick Airfoil Section Designed for General Aviation Applications," NASA TN D-7428, 1973.

55. Bonhaus, D., Anderson, K. and Mavriplis D., "Computed Flows of Sulfur Hexa-fluoride over Multi-element Airfoils," NASA TP to be published (1992).

56. Wilcox, D. C., "A Half-Century Historical Review of the  $k-\omega$  Model," AIAA Paper No. 91-0615, January 1991.

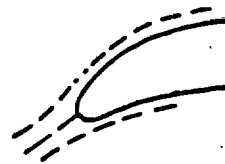


(a) Slat and single slotted flap (Ref.2)



(b) Slat and double slotted flap (Ref.4)

Figure 1: Examples of Multi-component Airfoil Configurations for Subsonic Transport High-lift Studies.



(a) Attached Flow Flap



(b) Vortex Flow Flap

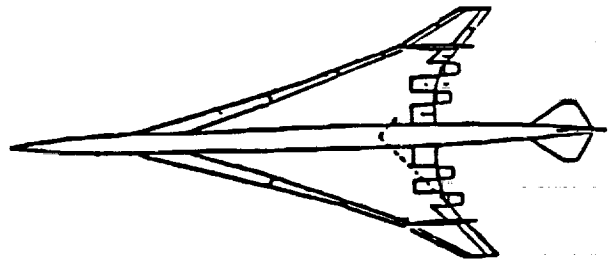
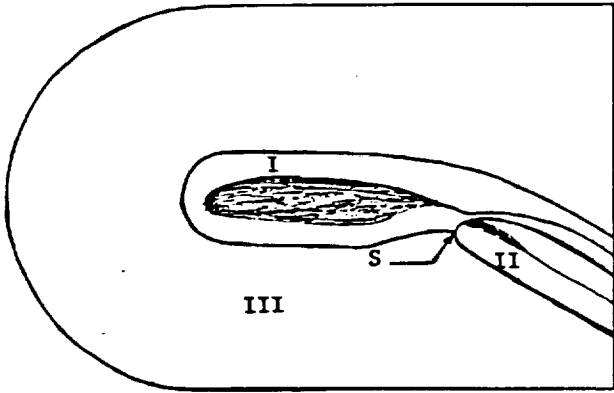
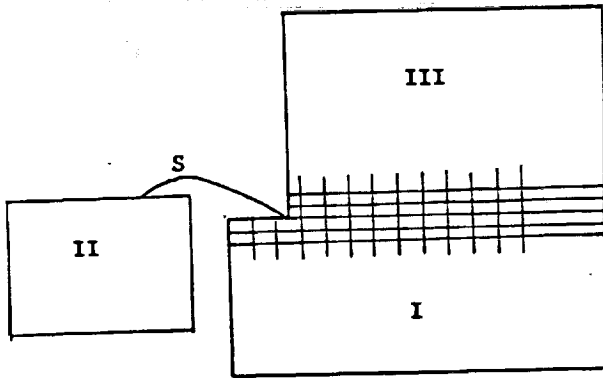


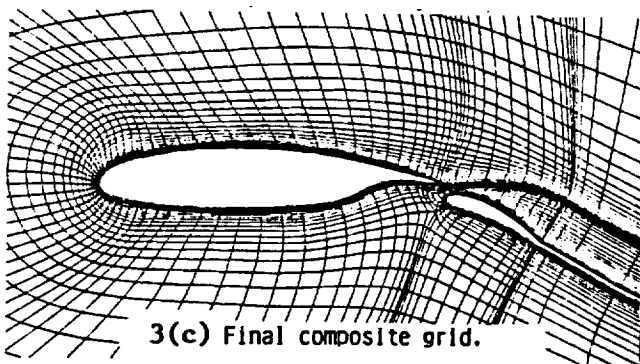
Figure 2: Schematic of a low aspect ratio highly swept arrow wing configuration with leading and trailing edge segmented flaps.



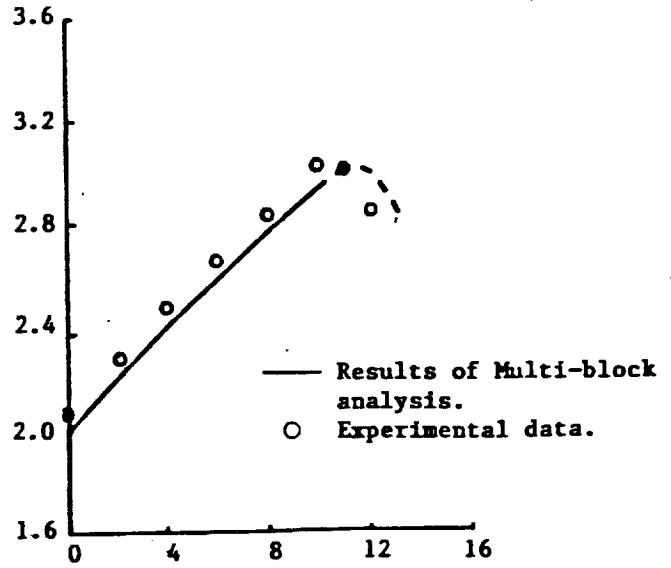
3(a) Patched grid system.



3(b) Patched computational space.

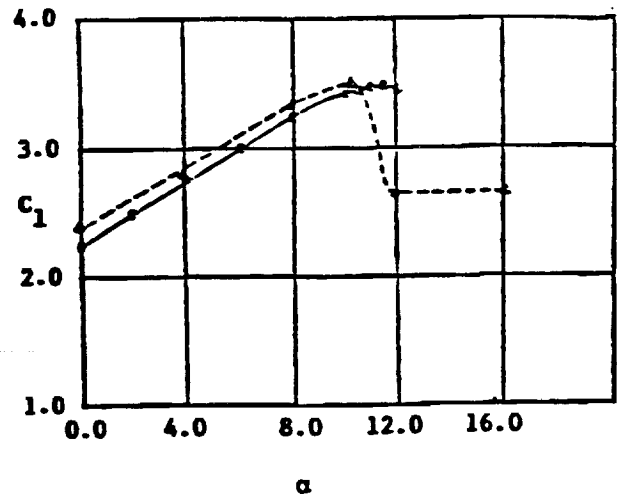


3(c) Final composite grid.



3(d)  $C_1$  vs  $\alpha$

Figure 3: Multi-block grid system and comparison of theoretical and experimental lift curves for a GAW-1 multi-element airfoil arrangement.



—○— Experimental results.  
 --△-- Computational predictions.

Figure 4:  $C_1$  vs  $\alpha$  for a multi-airfoil arrangement from Ref. 19.

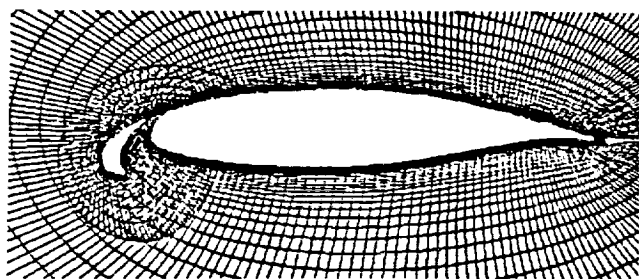
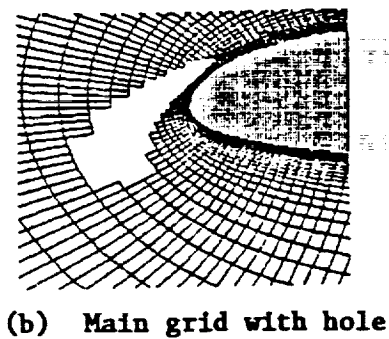
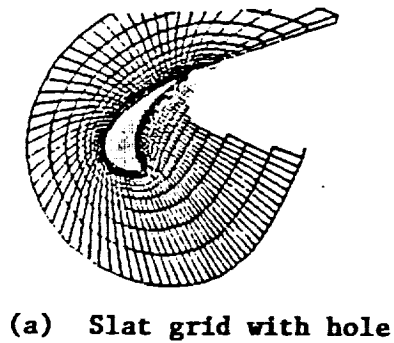
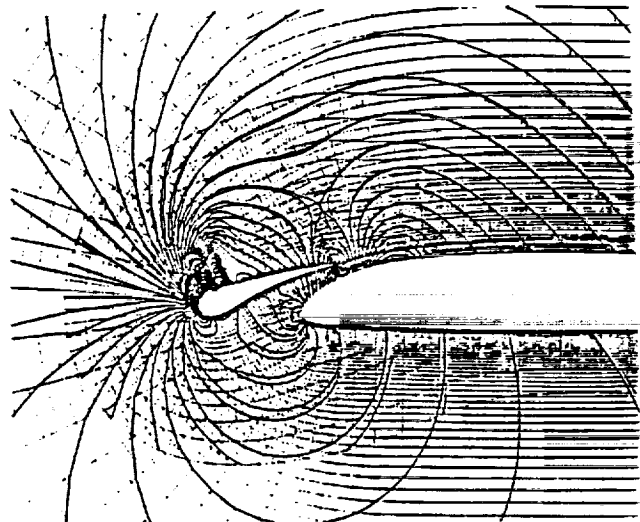


Figure 5: Chimera grid for a GAW-1 airfoil with deployed slat.

(a) Grid with Pressure Contours



(b) Surface Pressure Coefficient

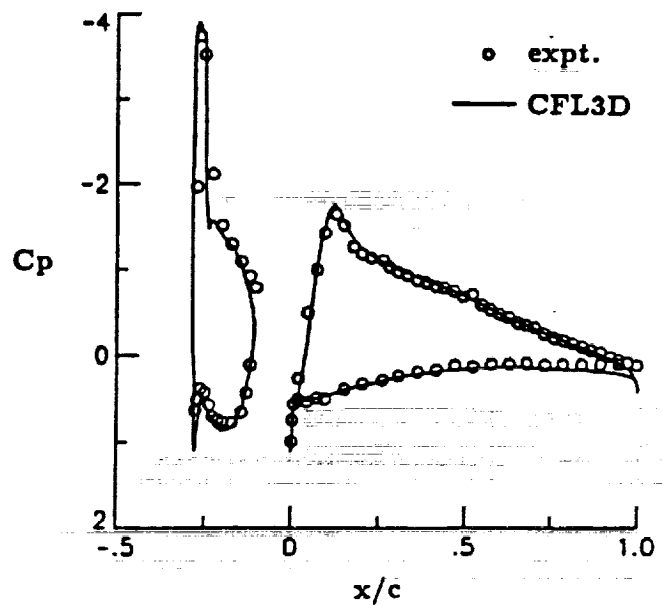
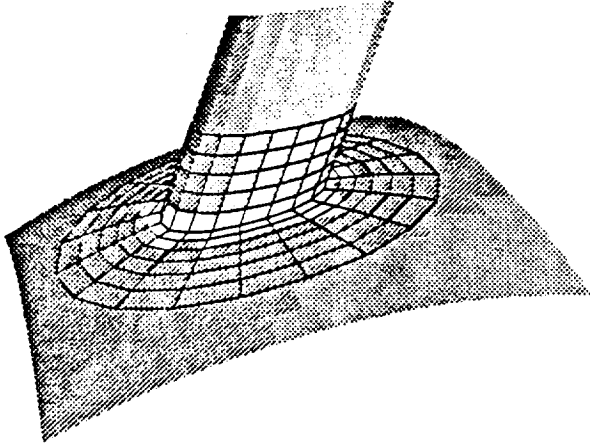
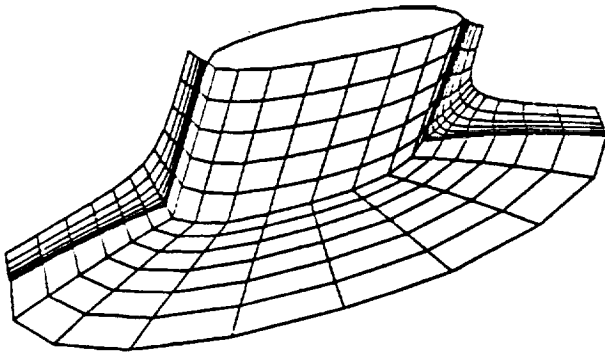


Figure 6: Euler solutions for an airfoil with slat at angle of attack,  $\alpha = 7.5^\circ$  and  $M_\infty = .5$  from Biedron. The calculations were obtained using CFL3D overlapped grid option.



(a)



(b)

Figure 7: An example of a "collar grid" for a cylinder intersecting a curved surface; (A simplified model of the Shuttle External Tank and liquid hydrogen feed line) from Ref. 34. (a) Combined collar surface grid; (b) Slices of the completed collar grid.

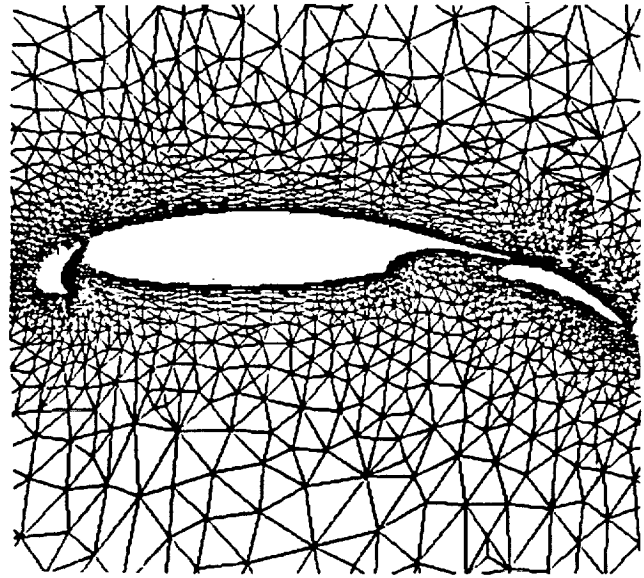
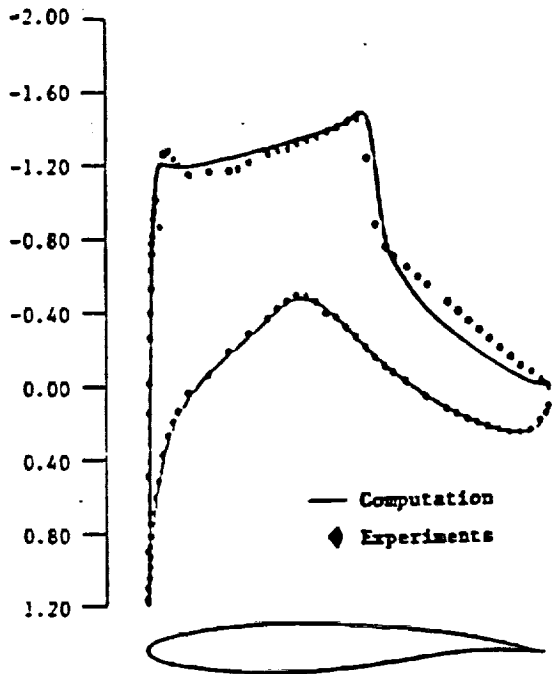


Figure 8: An unstructured mesh for computation of a GAW-1 multi-element airfoil configuration in a deployed state.

(a) RNG Turbulence Model



(b) Baldwin Lomax Model

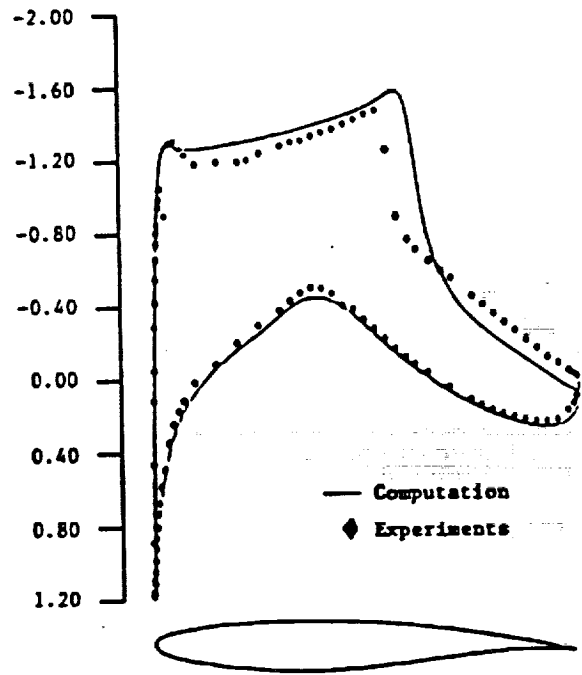


Figure 9: Comparison of RNG Turbulence Model and Baldwin Lomax Model for an RAE2822 airfoil at  $M_\alpha = 0.75$ ;  $R_\infty = 6.26 \times 10^6$  and  $\alpha = 2.8^\circ$  from Reference 49.

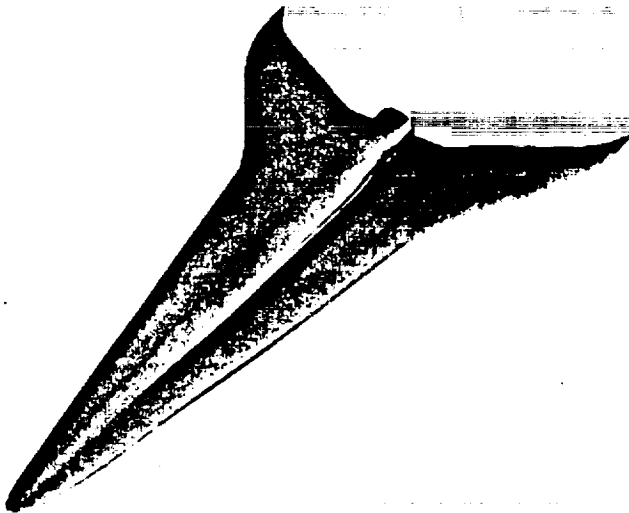


Figure 10a: Blended body HSCT configuration designed for  $M_\infty = 3.0$  cruise.

HSCT Configuration

Surface Pressure Distributions

$M_\infty = 0.3$ ,  $\alpha = 18^\circ$ ,  $Re_\infty = 4.4 \times 10^7$

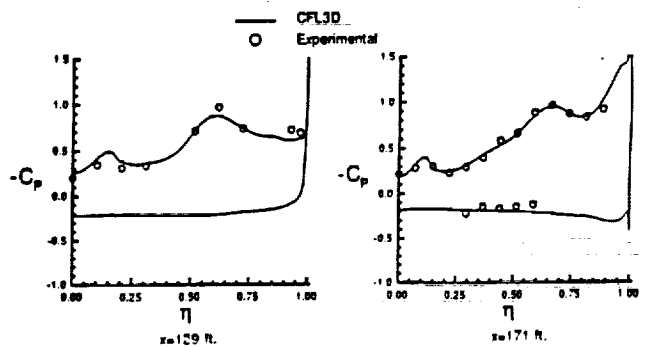


Figure 10b: Comparisons of surface pressure distribution for the HSCT configuration.

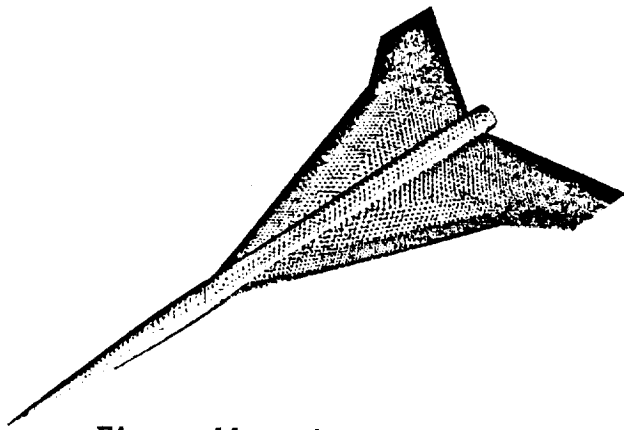


Figure 11a: An unstructured grid for a generic high speed research configuration.

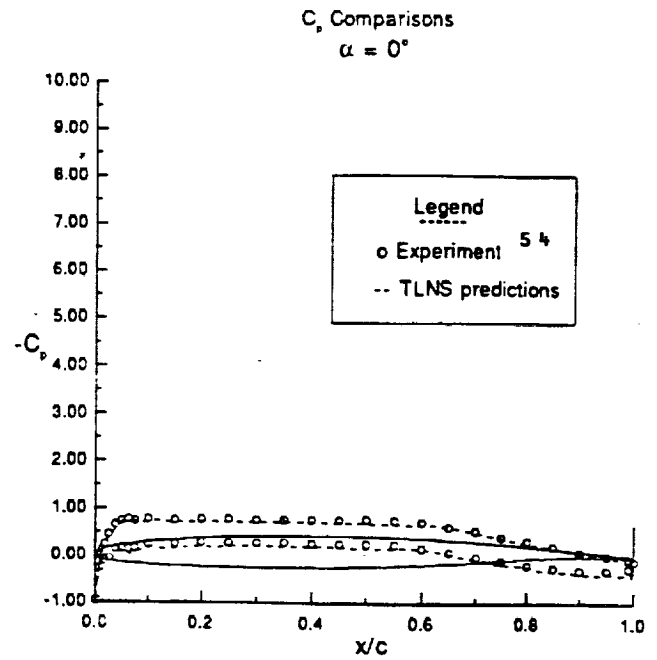


Figure 12a: Comparison of  $C_p$  for GAW-1 airfoil.

Generic HSR Configuration  
Mach = 0.2

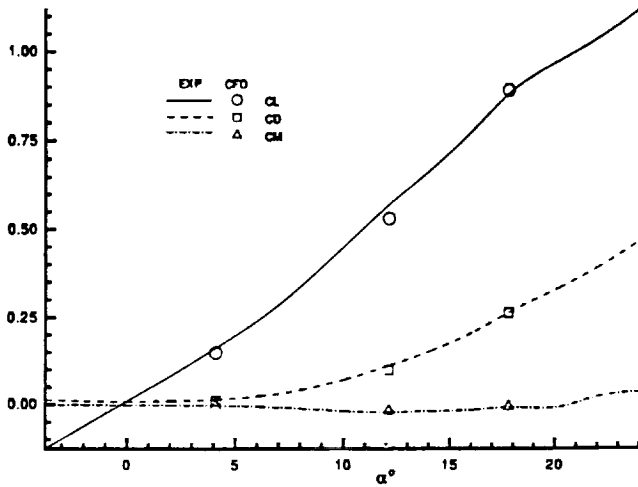


Figure 11b: Euler comparison of Lift, Drag, and Pitching moment for a generic HSR configuration.

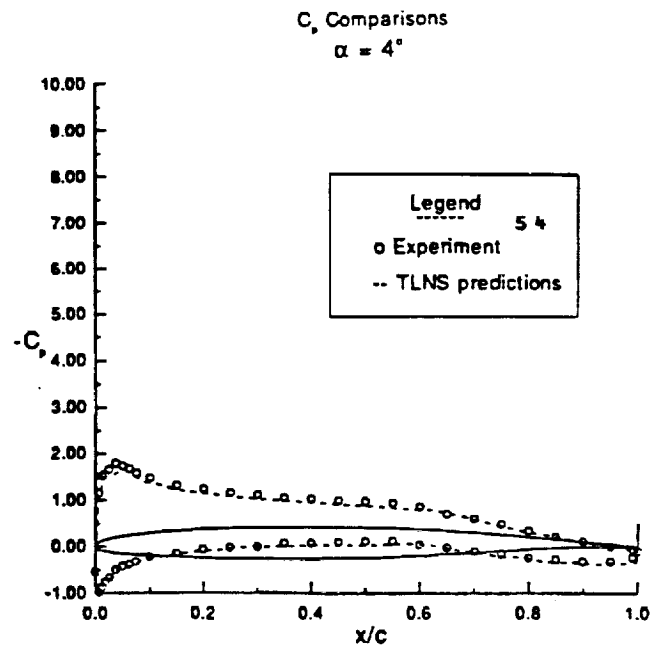


Figure 12b: Comparison of  $C_p$  for GAW-1 airfoil.

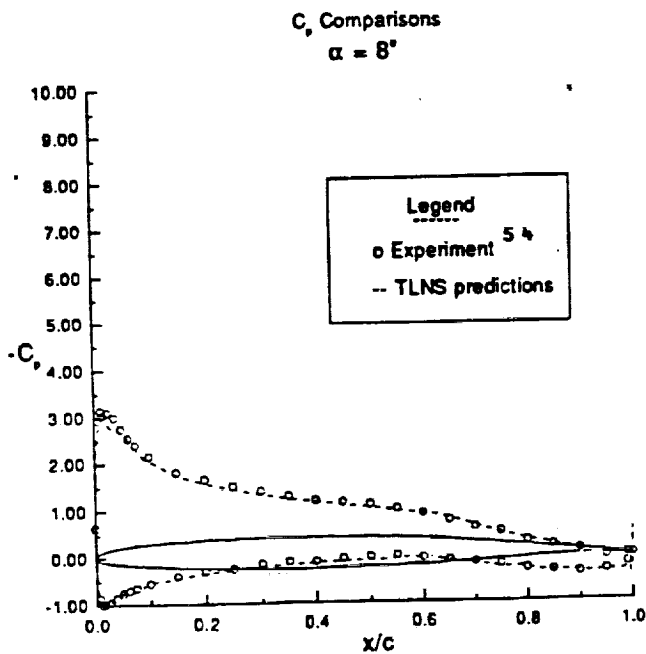


Figure 12c: Comparison of  $C_p$  for GAW-1 airfoil.

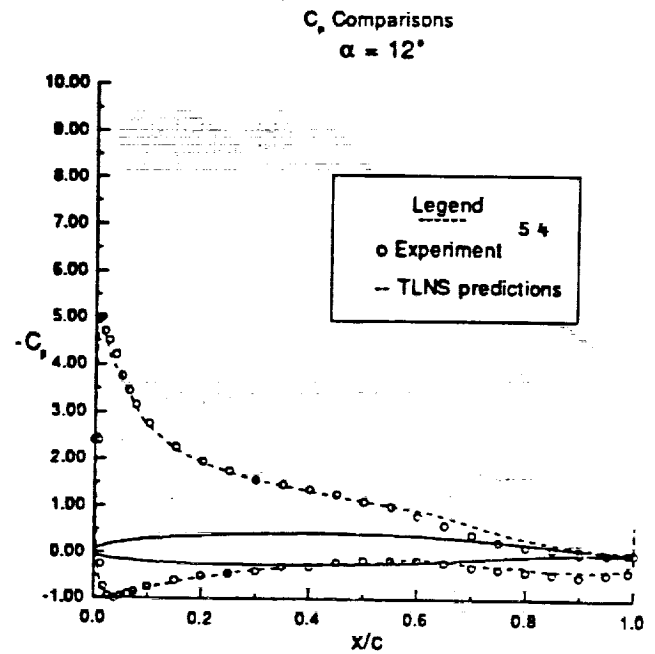


Figure 12d: Comparison of  $C_p$  for GAW-1 airfoil.

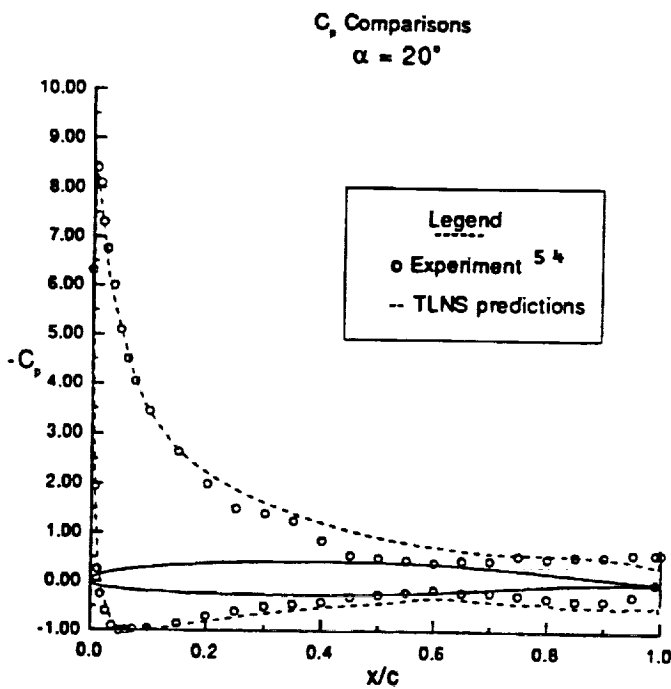


Figure 12f: Comparison of  $C_p$  for GAW-1 airfoil.

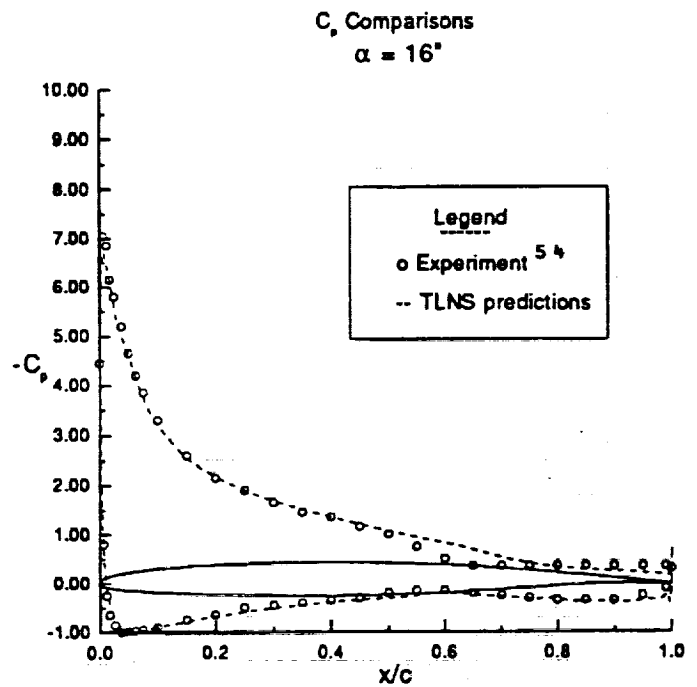


Figure 12e: Comparison of  $C_p$  for GAW-1 airfoil.

Variation of  $C_l$  vs  $\alpha$

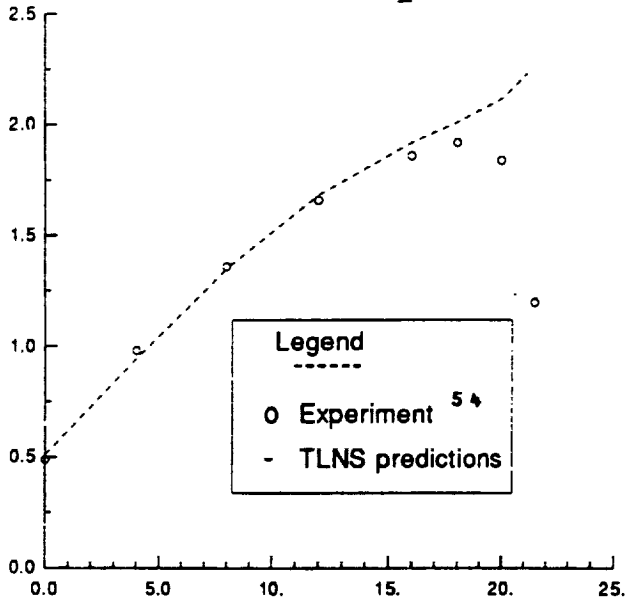


Figure 13: Comparison of  $C_l$  for GAW-1 airfoil.

Variation of  $C_d$  vs  $\alpha$

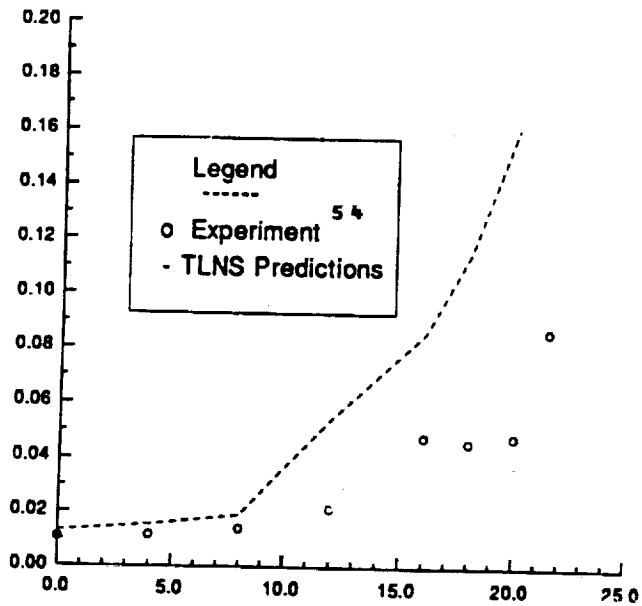


Figure 14: Comparison of  $C_d$  for GAW-1 airfoil.

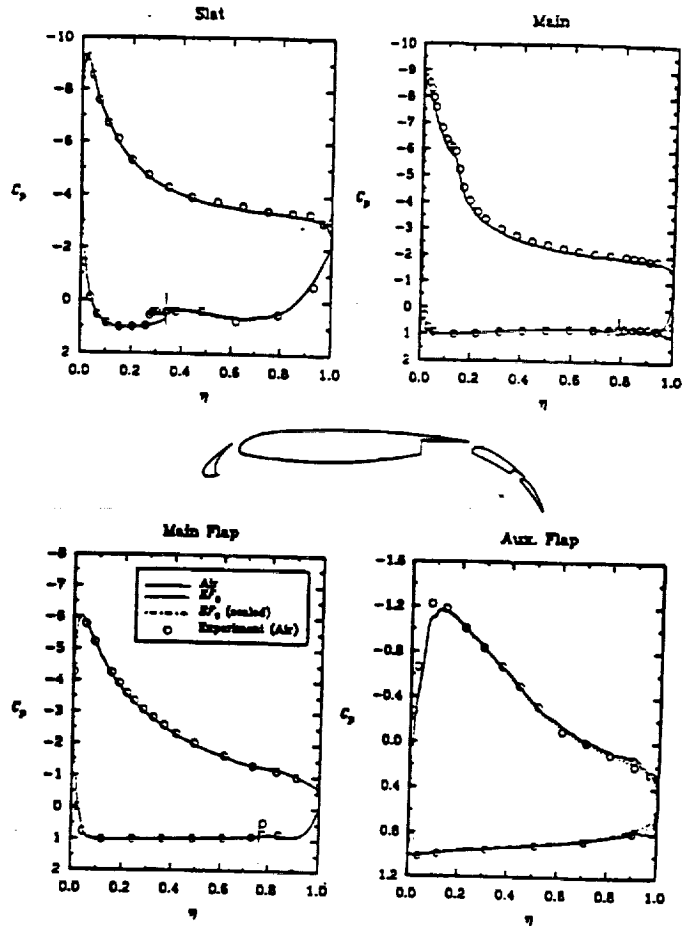


Figure 15a:  $C_p$  comparisons for a multi-element airfoil arrangement at  $M = .2$ , and with  $\alpha = 12^\circ$ .

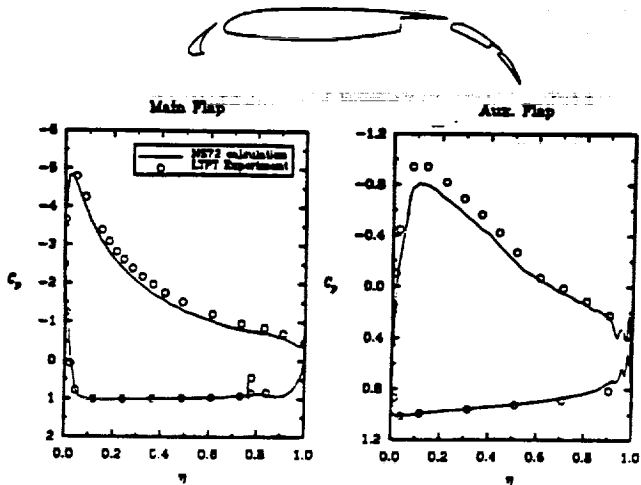
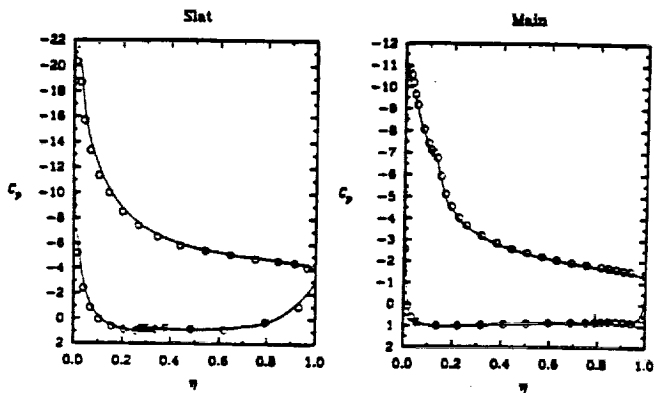


Figure 15b:  $C_p$  comparisons for a multi-element airfoil arrangement with  $\alpha = 20^\circ$ ,  $M_\infty = .2$

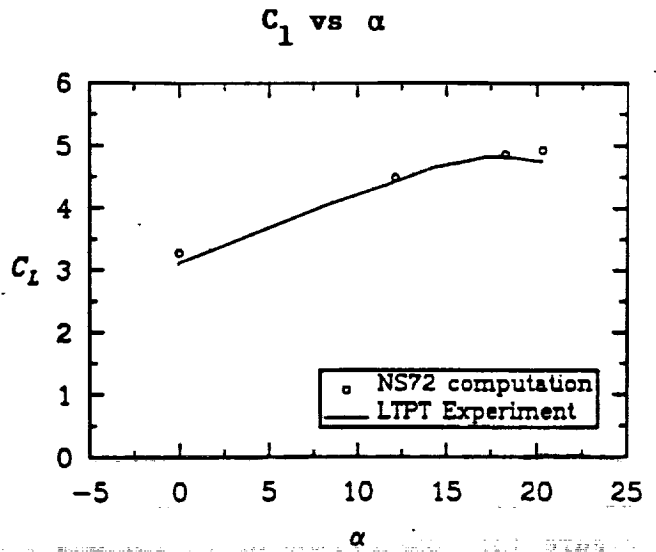


Figure 16:  $C_l$  vs  $\alpha$  comparisons for a multi-element configuration.

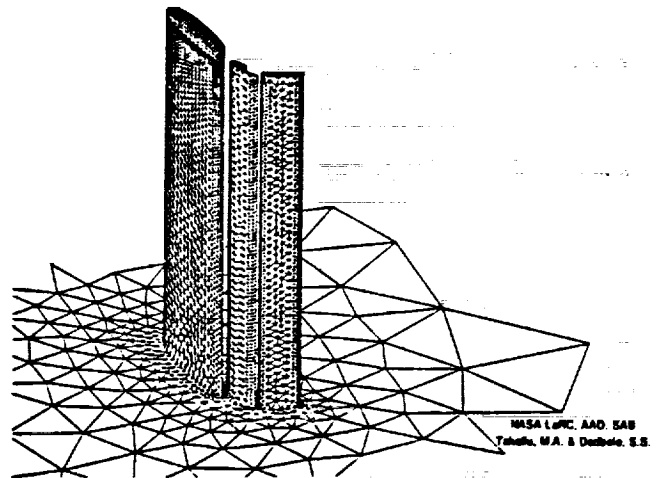
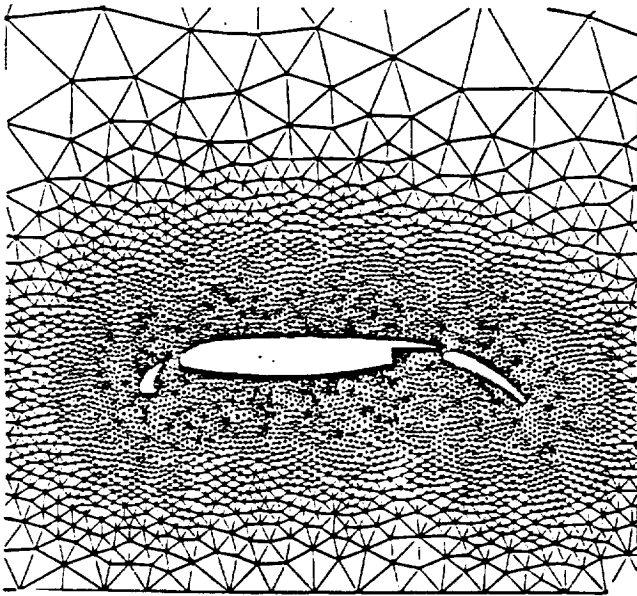
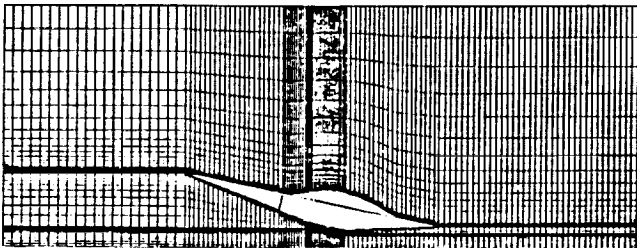


Figure 17: An example of a three-dimensional unstructured grid system for a semi-span high lift wing.



**Figure 18: Unstructured grid for a multi-component airfoil in ground effect study.**



**Figure 19: Cross section of a structured multi-block grid system for a high speed configuration in ground effects studies.**

